JACS
JOURNAL OF THE AMERICAN CHEMICAL SOCIETY
Article
pubs.acs.org/JACS

A Semisynthetic Strategy Leads to Alteration of the Backbone Amidate Ligand in the NiSOD Active Site

Julius O. Campeciño,[†] Lech W. Dudycz,[‡] David Tumelty,[§] Volker Berg,[†] Diane E. Cabelli,[∥] and Michael J. Maroney*[,†]

[†]Department of Chemistry University of Massachusetts, Amherst, Massachusetts 01003, United States
[‡]Lex Company Research Lab, Phoenix Park, 2 Shaker Road, Suite D 106, Shirley, Massachusetts 01464, United States
[§]New England Peptide, 65 Zub Lane, Gardner, Massachusetts 01440, United States
[∥]Department of Chemistry, Brookhaven National Laboratory, Building 555A, P.O. Box 5000 Upton, New York 11973, United States

Supporting Information

ABSTRACT: Computational investigations have implicated the amidate ligand in nickel superoxide dismutase (NiSOD) in stabilizing Ni-centered redox catalysis and in preventing cysteine thiolate ligand oxidation. To test these predictions, we have used an experimental approach utilizing a semisynthetic scheme that employs native chemical ligation of a pentapeptide (HCDLP) to recombinant *S. coelicolor* NiSOD lacking these N-terminal residues, NΔ5-NiSOD. Wild-type enzyme produced in this manner exhibits the characteristic spectral properties of recombinant WT-NiSOD and is as catalytically active. The semisynthetic scheme was also employed to construct a variant where the amidate ligand was converted to a secondary amine, H1*-NiSOD, a novel strategy that retains a backbone N-donor atom. The H1*-NiSOD variant was found to have only ∼1% of the catalytic activity of the recombinant wild-type enzyme, and had altered spectroscopic properties. X-ray absorption spectroscopy reveals a four-coordinate planar site with N_2S_2-donor ligands, consistent with electronic absorption spectroscopic results indicating that the Ni center in H1*-NiSOD is mostly reduced in the as-isolated sample, as opposed to 50:50 Ni(II)/Ni(III) mixture that is typical for the recombinant wild-type enzyme. The EPR spectrum of as-isolated H1*-NiSOD accounts for ∼11% of the Ni in the sample and is similar to WT-NiSOD, but more axial, with $g_z < g_{x,y}$. ^{14}N-hyperfine is observed on g_z, confirming the addition of the apical histidine ligand in the Ni(III) complex. The altered electronic properties and implications for redox catalysis are discussed in light of predictions based on synthetic and computational models.

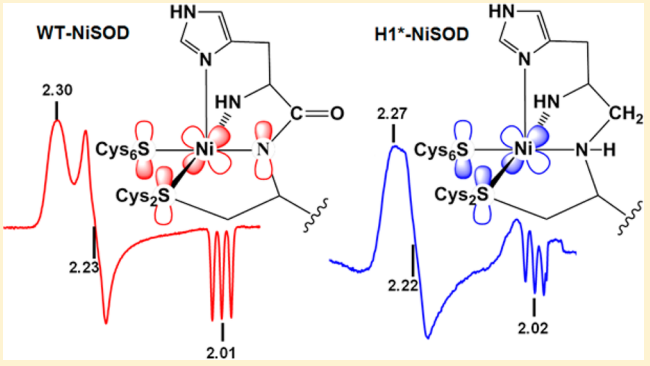

1. INTRODUCTION

Superoxide dismutases (SODs) comprise a class of ubiquitous metalloenzymes that catalyze the disproportionation of superoxide radical to molecular oxygen and hydrogen peroxide.[1,2] It is estimated that about 1−2% of the molecular oxygen consumed in the mitochondria is released as superoxide radical.[3] Thus, SODs are important regulators of free radicals and reactive oxygen species in the cell.[4]

There are three families of SODs based on protein structure and metal content: CuZnSOD, Fe/MnSOD, and NiSOD.[2] Of particular interest here is the nickel-dependent enzyme, NiSOD, which is expressed by the *sodN* gene, and commonly found in *Streptomyces* sp. and cyanobacteria. This gene encodes a pro-protein with an N-terminal extension that is cleaved in the mature enzyme, a required step for enzymatic activity.[5,6] NiSOD is unique among the SODs in that aquated Ni(II) ions are redox inactive under physiological conditions and do not catalyze superoxide disproportionation without the protein environment, unlike Cu(II), Fe(II), and Mn(II).[7] The NiSOD protein environment is used to lower the redox potential of the Ni(II/III) couple in the enzyme to near 300 mV,[8] the optimum value for SOD catalysis.[2] This is achieved in large part by the use of cysteine ligands in NiSOD[9−11] that are absent in the active sites of Fe/Mn- and CuZn-SODs.[2] The two cysteine thiolate ligands from Cys2 and Cys6 plus the N-terminal amine, His1 imidazole, and the Cys2 amidate N-donor, constitute the ligands in NiSOD active site. These ligands are used to form a five coordinate pyramidal Ni(III) site and a four-coordinate planar Ni(II) site that lacks the apical His1 imidazole ligand.[2] Thus, all the ligands used in forming the Ni site are derived from the first six amino acid residues, and four of the five are provided by His1 and Cys2.

Herein, we describe a semisynthetic strategy employing native chemical ligation (NCL) of a pentapeptide (HCDLP) to recombinant *Streptomyces coelicolor* NiSOD that lacks these five

Received: April 7, 2015
Published: July 1, 2015

DOI: 10.1021/jacs.5b03629
J. Am. Chem. Soc. 2015, 137, 9044−9052

N-terminal residues and features an N-terminal Cys residue (NΔ5-NiSOD) to produce a variant (H1*-NiSOD, Figure 1)

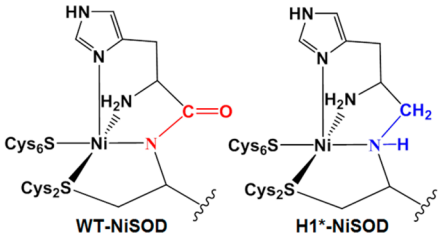

Figure 1. Nickel site structures of WT-NiSOD (left) and the H1*-NiSOD variant (right).

wherein the backbone Cys2 amidate N-donor ligand is altered to a secondary amine. Prior computational investigations of the NiSOD active site[12] as well as experimental and DFT calculations on model complexes,[13−16] predicted that the amidate ligand plays a role in the electronic structure of the Ni(III) site by keeping the oxidation product Ni-centered rather than S-centered, in contrast to the oxidation products of planar Ni(II) complexes with amine and thiolate ligation.[17−20] Characterization of the variant by X-ray absorption, EPR, and electronic absorption spectroscopies, and by reaction kinetics using pulse-radiolytically generated superoxide show that the variant has altered electronic structure and redox catalytic properties that are consistent with the roles of amidate ligation predicted by computations.

2. MATERIALS AND METHODS

2.1. Mutagenesis. The deletion mutant, NΔ5-NiSOD, was expressed using the pelB expression system.[11] The pelB WT-NiSOD construct was designed by isolating the WT-NiSOD gene previously inserted in pET-30 Xa/LIC vector[6] and reinserting the gene into the pET22b(+) upstream of the pelB sequence (Novagen protocol). This construct was then used as a template to construct a plasmid containing the NΔ5-NiSOD deletion mutant using the polymerase chain reaction (PCR). To delete the first five amino acids of the WT-NiSOD sequence (see Supporting Information, SI, Figure S1) the following primers were used: 5′-TGCGGCGTGTACGACCCTGC-3′ (forward primer) and 5′-GGCCATCGCCGGCTGGGC-3′ (reverse primer) with melting temperatures of 74 and 77 °C, respectively. The PCR was performed using Q5 high fidelity DNA polymerase (New England Biolabs Inc., Ipswich, MA) and only 1 pg of the template DNA. The denaturation temperature was 98 °C, and the annealing and extension temperature was 72 °C (NEB protocol). The PCR product was ligated without further purification by first adjusting the buffer using 5 μL of the 10X T4PNK reaction buffer (NEB) for every 45 μL of the PCR product. The sample was then treated with T4 DNA kinase followed by T4 DNA ligase (NEB protocol). To isolate the NΔ5-NiSOD plasmid, the ligated PCR product was transformed in NovaBlue cells and selection was performed using an LB agar plate containing 100 μg/mL ampicillin. Single colonies were picked and each colony was grown in 5 mL LB media with ampicillin for 16 h at 37 °C. The cultures were harvested, and plasmid preparation was performed using a Qiagen (Valencia, CA) kit. The sample plasmids were then submitted to Genewiz (South Plainfield, NJ) for sequencing. The plasmids with the correct sequence were stored at −20 °C for future use.

2.2. NΔ5-NiSOD Protein Expression and Purification. The pelB NΔ5-NiSOD plasmid was transformed into BL21 (DE3) and selected for ampicillin resistance on an LB agar plate supplemented with ampicillin. Single colonies were selected and grown in 5 mL LB media for 16 h at 37 °C @ 200 rpm and used to prepare frozen stocks by storing 1 mL aliquots in 50% glycerol at −80 °C. From a frozen stock, cultures were prepared in 150 mL LB medium supplemented with ampicillin and grown for 16 h at 37 °C @ 200 rpm. Aliquots (20 mL) from the culture were used to inoculate flasks containing 2 L of LB medium supplemented with ampicillin (total of six) and grown at 25 °C until 0.5 OD is reached. At this point, 200 μL of 1 M IPTG was added to each 2 L culture, and they were incubated for another 12 h at 25 °C. The culture was then harvested by centrifugation.

To extract NΔ5-NiSOD, the cells were disrupted by osmotic shock. This was done by resuspending the cells in 30 mM Tris buffer at pH = 8.00 containing 20% sucrose (50 mL total volume of per 2 L cell culture). After 10 min, the cells were centrifuged, the supernatant was discarded, and the cells were resuspended in water (50 mL total volume per 2 L culture) at 4 °C for another 10 min. The cells were again centrifuged, the pellet was discarded, and 200 μL of 200 mM PMSF was added per 50 mL of the supernatant. After 30 min, cysteine was added to the supernatant to a final concentration of 100 mM, and the solution was stored at 4 °C overnight to allow the cysteine to form a disulfide bond with the cysteine N-terminus of the NΔ5-NiSOD, thereby protecting the N-terminal cysteine from oxidation.

The NΔ5-NiSOD was purified using Q-sepharose resin packed in XK 16 column with resin height of 41 cm. The buffer used was 50 mM Tris at pH 8.50 and the NaCl concentration was linearly increased from 0 to 200 mM over 1500 at 3 mL/min. PAGE was performed to determine the fractions that contain pure NΔ5-NiSOD. The purified protein was characterized by mass spectroscopy (see SI Figure S2), which showed the presence of NΔ5-NiSOD (12634 Da) and impurities that correspond to N-terminally modified forms of NΔ5-NiSOD, principally the thiazolidine modification resulting from reaction with acetaldehyde (12661 Da).

2.3. NΔ5-NiSOD Chemical Rescue. Almost half of the NΔ5-NiSOD isolated as described above has the cysteine N-terminus reacted with endogenous acetaldehyde forming a thiazolidine ring structure.[21] To rescue the modified N-terminal cysteine, the protein was incubated at 37 °C at a final concentration of 1 mM in a solution containing 100 mM semicarbazide in 6 M guanidine HCl with 30 mM TCEP unbuffered at pH 4.00 for 1−2 h.[22] This procedure reverses the thiazolidine cyclization. The sample was then added to an equivalent volume of 1 M cysteine in 50 mM Tris buffer with 6 M guanidine hydrochloride at pH 7.50 and left for 4 h to overnight to allow the cysteine to replace the bound aldehyde via nucleophilic substitution (see SI Figure S3). This procedure was done twice to remove most of the aldehyde. Prior to the native chemical ligation, the cysteine bound at the N-terminus was removed by buffer exchanging the sample with 50 mM Tris pH 7.50 containing 30 mM TCEP at room temperature. The sample buffer was then exchanged with the ligation buffer (section 2.5) and stored at −20 °C for future use. The molecular weight of the product was determined by ESI-mass spectrometry: Found: 12634 Da. Calculated for NΔ5-NiSOD:12635 Da (see SI Figure S4). Yield: 50% of the protein from step 1.2 is recovered.

2.4. His-Cys(*o*-NBn)-Asp-Leu-Pro-Nbz (Protected Unmodified HCDLP). *2.4.1. Synthesis of Alloc-Cys(o-NBn)—OH.* Cys(*o*-NBn)—OH was first synthesized by dissolving 15 mmol cysteine in deaerated aqueous solution of 10 mmol potassium carbonate in 20 mL water 10 mL dioxane and treated with 10 mmol *o*-nitrobenzyl chloride. Formation of a crystalline product was observed after 30 min and after 4 h, the pH of the reaction mixture was adjusted to 5.9 with acetic acid. The product was collected by filtration and washed with water, isopropanol, and ether. The solids were dried under vacuum and a yield of 2.06 g (79%) of the product was obtained at 99% purity.

Alloc-Cys(*o*-NBn)—OH was then synthesized as previously described.[23] About 100 mmol of cysteine was dissolved in 2 mL of 4 N NaOH. The solution was cooled in an ice-bath and treated with 10.6 mL of allyl chloroformate and 25 mL of 4 N sodium hydroxide, added in eight equal portions with vigorous shaking for a few minutes after each addition, and intermittent cooling. The reaction mixture was kept alkaline to phenolphthalein throughout. After the last addition, the mixture was shaken vigorously, allowed to stand for 15 min at room temperature, extracted with ether, and then acidified to congo red with concentrated hydrochloric acid. After cooling for several hours, the product that crystallized was collected, dried, and recrystallized.

DOI: 10.1021/jacs.5b03629
J. Am. Chem. Soc. 2015, 137, 9044−9052

2.4.2. His-Cys(o-NBn)-Asp-Leu-Pro-Nbz SPPS Assembly. The pentapeptide His-Cys(*o*-NBn)-Asp-Leu-Pro-Nbz was assembled by Fmoc SPPS using 0.2 mmol of the commercially available Dawson Dbz AM resin. The C-terminal Pro was loaded onto the resin via two 1-h couplings using 1.2 mmol of Fmoc-Pro with activation via 1.2 mmol HATU and 1.8 mmol DIEA in DMF. Subsequent residues, Leu, Asp(OtBu) and Alloc-Cys(*o*-NBn) were coupled similarly using HBTU in place of HATU. The peptidoresin was protected from light after incorporation of the Alloc-Cys(*o*-NBn) residue. The Alloc protective group was removed by adding $(PPh_3)_4Pd(0)$ with 1,3-dimethylbarbituric acid (scavenger) to the peptide under neutral conditions. The final residue was incorporated using Boc-His(Trt)—OH.

After chain assembly, the resin was gently agitated with 2 mmol of *p*-nitrophenylchloroformate in DCM for 1 h to convert the resin to the N-acyl-benzimidazolinone (Nbz) form, which was then washed with DCM. The resin was agitated with 0.5 M DIEA in DMF for two 30 min treatments, then rinsed with the same solution until no further yellow coloration (from *p*-nitrophenol release) was observed. The peptidoresin was washed with DMF, MeOH, DCM then dried overnight in vacuo. The peptide was cleaved from the resin with trifluoroacetic acid/water/triisopropylsilane (90:5:5, 25 mL, 3 h) then precipitated in ice-cold ether. The crude peptide was purified by RP-HPLC to yield the final product (120 mg).

2.5. His-ψ-Cys(*o*-NBn)-Asp-Leu-Pro-SBn Synthesis (Modified H1*-CDLP). *2.5.1. Boc-His(N$^{\pi}$-Adom)-H Synthesis.* Protected histidinal, Boc-His(N$^{\pi}$-Adom)-H, was prepared by first synthesizing Boc-His(N$^{\pi}$-Adom)-OMe. This was accomplished by reacting 2-adamantyloxymethyl chloride with Boc-His(N$^{\pi}$-Boc)-OMe as described by Okada et al.[24] The product (Boc-His(N$^{\pi}$-Adom)-OMe) was then converted to Boc-His(N$^{\pi}$-Adom)-ol by first dissolving 10 mmol Boc-His(N$^{\pi}$-Adom)-OMe in 100 mL THF containing 60 mmol sodium borohydride. Methanol (16 mL) was then added dropwise followed by heating the solution at 40 °C. The progress of the reaction was monitored by HPLC on a C18 column. When the reaction was completed, excess sodium borohydride was removed by the addition of aqueous solution of citric acid. The resulting solution was concentrated until most of the organic solvent had been evaporated. The pH was then adjusted to 9 using potassium carbonate and the product (Boc-His(N$^{\pi}$-Adom)-ol) was extracted using dichloromethane. The product was obtained as white foam (3.4 g) with 98% purity (HPLC).

The alcohol (Boc-His(N$^{\pi}$-Adom)-ol) was then converted to the aldehyde, Boc-His(N$^{\pi}$-Adom)-H. This was done by dissolving 3.6 mmol Boc-His(N$^{\pi}$-Adom)-ol in 100 mL dichloromethane followed by dropwise addition of 1.7 eq Dess-Martin reagent. The progress of the reaction was monitored by HPLC and when the reaction was completed, the solution was treated with 10 mmol thiosulfate in 25 mL 10% bicarbonate buffer. The solution was concentrated until most of the organic solvent was removed and the material was used without any further purification.

2.5.2. His-ψ-Cys(o-NBn)-Asp-Leu-Pro-SBn SPPS Assembly. The pentapeptide benzylthioester, His-ψ-Cys(*o*-NBn)-Asp-Leu-Pro-SBn, was assembled by first synthesizing Alloc-Cys(*o*-NBn)-Asp(OtBu)-Leu-Pro by standard SPPS on 2-chlorotrityl resin. The cysteine N-terminal allyl carbamate (Alloc) protective group was then removed as before (section 2.4). The resulting peptide, Cys(*o*-NBn)-Asp(OtBu)-Leu-Pro, was then cleaved from the resin using acetic acid-trifluoroethanol-dichloromethane (1:2:7, v/v).

Reductive alkylation was then performed in solution to synthesize Boc-His(N$^{\pi}$-Adom)-ψ-Cys(*o*-NBn)-Asp(OtBu)-Leu-Pro—OH. This was done by dissolving 1.7 mmol Cys(*o*-NBn)-Asp(OtBu)-Leu-Pro and 1.6 equiv of Boc-His(N$^{\pi}$-Adom)-H in 30 mL methanol containing 0.3 mL acetic acid. The resulting solution was then treated with 4 eq sodium cyanoborohydride in portions. The reaction went to 90% completion (HPLC) after which methanol and acetic acid were then removed by evaporation under vacuum. The product, (Boc-His(N$^{\pi}$-Adom)-ψ-Cys(*o*-NBn)-Asp(OtBu)-Leu-Pro—OH), was then suspended in citric acid solution and extracted with dichloromethane, and then concentrated without further purification.

To the crude 1.68 mmol Boc-His(N$^{\pi}$-Adom)-ψ-Cys(*o*-NBn)-Asp(OtBu)-Leu-Pro—OH solution, 9 mmol benzyl mercaptan was added together with 0.2 mmol DMAP hydrochloride and 0.26 eq DMAP in 30 mL dichloromethane. The resulting solution was treated with 2.14 mmol EDC for 1 h, after which the reaction was quenched with phosphate buffer at pH 6. The solution was then concentrated and the excess benzyl mercaptan was removed by washing the residue with heptane. The remaining material was then dissolved in dichloromethane and washed with phosphate buffer. The crude peptide was further purified using FC silica gel yielding 0.94 g material with ∼80% purity. Treatment of the product with TFA/water (95:5) for an hour cleanly removed acid-sensitive protecting groups, Boc, tBu, and Adom. The target peptide was finally purified on reverse phase column in TFA-containing gradient of water and acetonitrile and then lyophilized.

2.6. Native Chemical Ligation and Product Purification. The native chemical ligation was performed by combining 6 mM pentapeptide and 3 mM NΔ5-NiSOD in 100 mM phosphate buffer with 6 M guanidine hydrochloride, 15 mM TCEP and 250 mM 4-mercaptophenylacetic (MPAA) acid at pH = 7.00 for 24 h at room temperature in an anaerobic chamber (Coy Laboratories Inc., Grass Lake, MI). The ligation product is a mixture of properly ligated H1*-NiSOD as well as NΔ5-NiSOD oxidized at the N-terminal Cys residue, and NΔ5-NiSOD that had been desulfurized by reaction with TCEP[25] (SI Figure S5). The properly ligated protein was purified from the oxidized and desulfurized NΔ5-NiSOD, which both lack a thiol group, by using activated thiol sepharose affinity column chromatography. First, the NCL buffer was exchanged with a binding buffer consisting of 100 mM Tris, 8 M guanidine hydrochloride, 500 mM NaCl, and 1 mM EDTA at pH = 7.50. This step also removes the excess MPAA that might interfere with the purification process. Next, the protein was loaded on to a column containing 1 mL of activated thiol sepharose resin and incubated at room temperature for at least 2 h. The column was then washed with 30 mL of the binding buffer to remove unbound proteins. The bound protein was then eluted with 10 mM Tris containing 50 mM β-mercaptoethanol at pH= 7.50 (SI Figure S6).

2.7. Cys2 Protective Group Removal, Folding and Metalation. To remove the 2-nitrobenzyl protecting group, 50 μM protein in a buffer consisting of 100 mM sodium acetate, 20 mM TCEP, and 10 mM semicarbazide at pH 5.80 was placed in an ice bath and irradiated with UV light at 365 nm. The extent of the reaction was monitored by mass spectrometry, and the reaction is complete after 4 h of irradiation. The sample was then dialyzed at 4 °C against 20 mM Tris buffer containing 5 mM TCEP and 5 mM $NiCl_2$ at pH 8.00 overnight. The sample was then dialyzed at 4 °C against 20 mM Tris at pH 8.00 for 12 h, twice. Finally, the sample was treated with Chelex to remove any unbound nickel by adding a small amount of chelex resin and incubated at room temperature for 30 min and agitated occasionally. The Ni/protein ratio was determined by analyzing the nickel and sulfur content of the sample by ICP-OES. The ICP-OES determination of the enzyme concentration was done by first making a standard curve using 2, 5, 10, 20, and 50 ppm sulfur standards prepared from a 1000 ppm sulfur ICP standard (Sigma-Aldrich). The concentration of sulfur in each sample was then determined using the standard curve (machine automated determination). The protein concentration was calculated by dividing the sulfur concentration by 3 (since NiSOD has two cysteines and one methionine). Yield: 600 μg protein from 10 mg prior to native chemical ligation.

2.8. X-ray Absorption Spectroscopy. A 50-μL sample containing 3 mM enzyme (per nickel basis) in 20 mM Tris buffer at pH = 8.00 was treated with 10 μL of 180 mM dithionite for 1−2 min in a coy chamber (Coy Laboratory Products Inc., Grass Lake, MI). The sample was then added with 10 μL of glycerol (∼15% final concentration) and loaded into a polycarbonate XAS holder wrapped in Kapton tape and slowly frozen in liquid nitrogen.

Ni K-edge XAS data were collected as previously described[26] at 10 K using a liquid helium cryostat (Oxford Instruments) on beamline 7−3 at the Stanford Synchrotron Radiation Laboratory (SSRL). The data were collected at ∼10 K using a liquid helium cryostat (Oxford

DOI: 10.1021/jacs.5b03629
J. Am. Chem. Soc. 2015, 137, 9044−9052

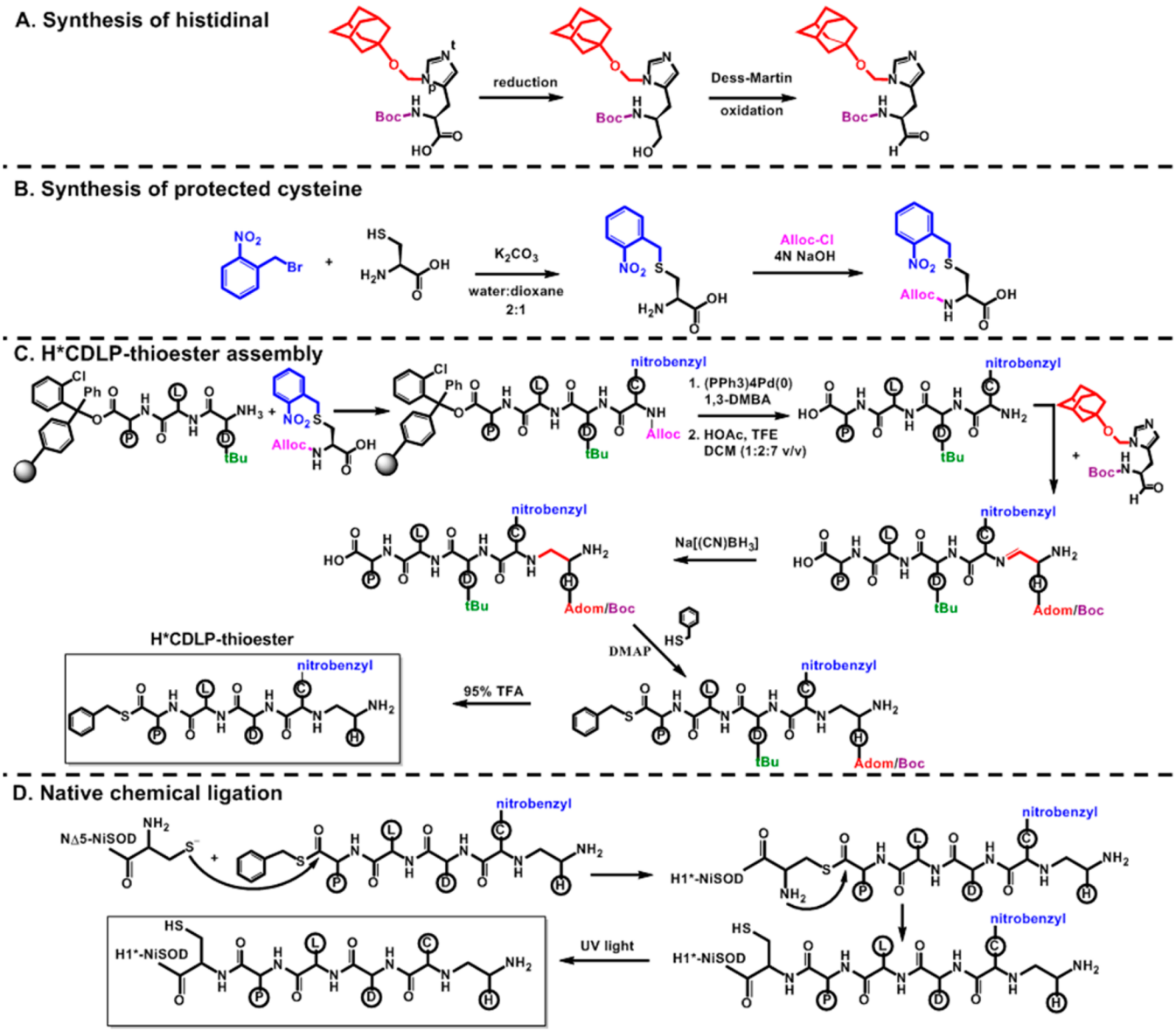

Figure 2. Semisynthetic approach for constructing H1*-NiSOD.

Instruments) under ring conditions of 3 GeV and 495−500 mA. Beamline optics consisted of a Si(220) double-crystal monochromator and a flat rhodium-coated mirror before the monochromator for harmonic rejection and vertical collimation. X-ray fluorescence was collected using a 30-element germanium detector (Canberra). Scattering was minimized by placing a set of Soller slits with a Z-1 element filter between the sample chamber and the detector. Internal energy calibration was performed by collecting spectra simultaneously in transition mode on nickel foil to determine the first inflection point on the edge, which was set to 8331.6 eV.

Sixpack software was used to remove bad detector signals, and calibrate the edge energy of Ni foil, and finally to average the data. Athena software was used for data reduction and normalization. This was done by setting E_0 = 8340 eV, R_{bkg} to 1.0, and spline range from k = 0 Å to k = 16.166 Å. Background subtraction and edge normalization was performed by setting the pre-edge range from −200 to −30 eV relative to E_0, and the postedge was set from 200−896 eV relative to E_0.

EXAFS data were analyzed using the Artemis software as previously described.[27] The k^3-weighted data were fitted by setting the FT-window to 2.0−12.5 Å and fitting from r = 1.25−2.3 Å in r-space with an S_o value of 0.9. Fits of first-coordination sphere scattering atoms were obtained with the following combinations of first-shell scattering atoms: 4N; 3N, 1S; 2N, 2S; 1N, 3S; and 4S. The 2N, 2S combination afforded the best fit, judged by minimizing the values of the R-factor and reduced χ^2, with the 2N-scattering and 2S-scattering atoms each averaged in single shells. When it became apparent that the H1*-NiSOD active site is structurally similar to WT-NiSOD, second shell carbon atoms from the five-membered chelate rings formed by His1 and Cys2 were added to the fit, and the fitting range was extended to r = 1.25−4.5 Å. The WT-NiSOD active site crystal structure (PDB: 1Q0G) was used as model for calculating theoretical phase and amplitude parameters using FEFF 6.0 including multiple-scattering for second coordination sphere C atoms.

XANES analysis was performed in the energy range from 8325 to 8340 eV using an error function centered at 8340 eV to fit a portion of the edge background, and Gaussian functions centered at 8331 eV to fit the 1s → 3d transition and at 8336 eV to fit the 1s → 4p_z transition (see SI Figure S7).

2.9. UV−vis Spectroscopy. UV−vis absorption spectra of the recombinant WT-NiSOD, dithionite-reduced WT-NiSOD, semi-synthetic WT-NiSOD, and H1*-NiSOD were obtained using a NanoDrop 2000c spectrophotometer. The absorption coefficients were calculated using the enzyme concentration calculated based on

DOI: 10.1021/jacs.5b03629
J. Am. Chem. Soc. 2015, 137, 9044−9052

the sulfur content of the sample as determined by ICP-OES (vide supra).

2.10. Electron Paramagnetic Resonance Spectroscopy. The EPR spectra were obtained using a Bruker Elexsys E500 cw-X-band EPR spectrometer. About 100 μL of a 200−1000 μM solution of each sample was loaded in EPR tubes and frozen using liquid nitrogen. The magnetic field is centered at 3200 G with a sweep width set to 1500 G. The modulation frequency was set to 100 kHz, while the modulation amplitude was set to 2 G. The receiver gain of 60 dB and attenuation of 10 db were applied and a time constant and conversion time of 0.64 and 655 ms were used, respectively. Spectral smoothing and baseline correction was performed using SpinCount software (M. Hendrich).

Spin integration of the EPR signal from H1*-NiSOD was performed by comparing the double integration of the first derivative signal vs a Cu(II) standard (1.0 mM $CuSO_4$ in 2 M $NaClO_4$ and 10 mM HCl), where the Cu content was determined by ICP-OES.

2.11. Pulse Radiolysis. The catalytic activities of the semisynthetic WT-NiSOD and H1*-NiSOD were determined by pulse radiolysis using a 2.0 MeV van de Graaff accelerator at Brookhaven National Laboratory, as previously described.[8] Micromolar concentrations of the semisynthetic enzymes were exposed to short pulses (100−600 ns) of highly accelerated electrons producing 2−10 μM of superoxide radical. The catalytic activity was measured by monitoring the rate of disappearance of superoxide radical absorption at 260 nm in a buffered solution containing 2 μM protein (per nickel basis), 10 mM phosphate, 30 mM formate, and 5 μM EDTA at pH 7.50. Rates of reaction are reported on a per Ni basis and assume that all of the Ni in the sample is catalytically active. All quoted rates represent the average of at least three individual measurements and the system error is approximately 10%.

3. RESULTS

3.1. Semisynthesis. A semisynthetic approach (Figure 2) was used to produce a variant of NiSOD in which the backbone amidate ligand provided by Cys2 is altered to a secondary amine. The semisynthesis of WT-NiSOD was carried out as a control using NCL to couple a pentapeptide comprising the five N-terminal amino acids to a truncated NiSOD with an N-terminal Cys residue, NΔ5-NiSOD, which was produced recombinantly. A key feature of the approach is the use of a photolabile thiol protecting group (2-nitrobenzyl) that was used to protect Cys2 in order to keep it protected during NCL after acid deprotection of other residues, and also distinguish it from the N-terminal Cys of NΔ5-NiSOD. Following NCL and purification of the product, the 2-nitrobenzyl protecting group was removed photochemically by exposing the sample with UV light at 365 nm. The production of the semisynthetic WT-NiSOD protein was confirmed by ESI-MS performed under denaturing conditions (Figure 3A). The sample was then folded and nickelated. Nickel and protein (sulfur) content were determined by ICP-OES and gave a nickel loading of 84%. The resulting enzyme was found to be a fully active catalyst (vide infra) and was hexameric according to size exclusion chromatography (SI Figure S8).

The synthesis of the H1*-NiSOD variant was accomplished in an analogous manner to the semisynthesis of WT-NiSOD. The pentapeptide benzylthioester was prepared using SPPS and Alloc-*S*-*o*-nitrobenzyl cysteine, as before. The desired amide → amine modification was introduced in solution after cleavage of the tetrapeptide (CDLP) from the resin by using the aldehyde, histidinal, instead of the natural amino acid histidine to produce an imine linkage that was then converted to secondary amine by reduction with $Na[(CN)BH_3]$ (Figure 2C). The synthesis of *δ*-*N*-adamantyl-*O*- and Boc-protected histidinal from the corresponding protected histidine was achieved by reduction of the amino acid to the alcohol followed by Dess-Martin

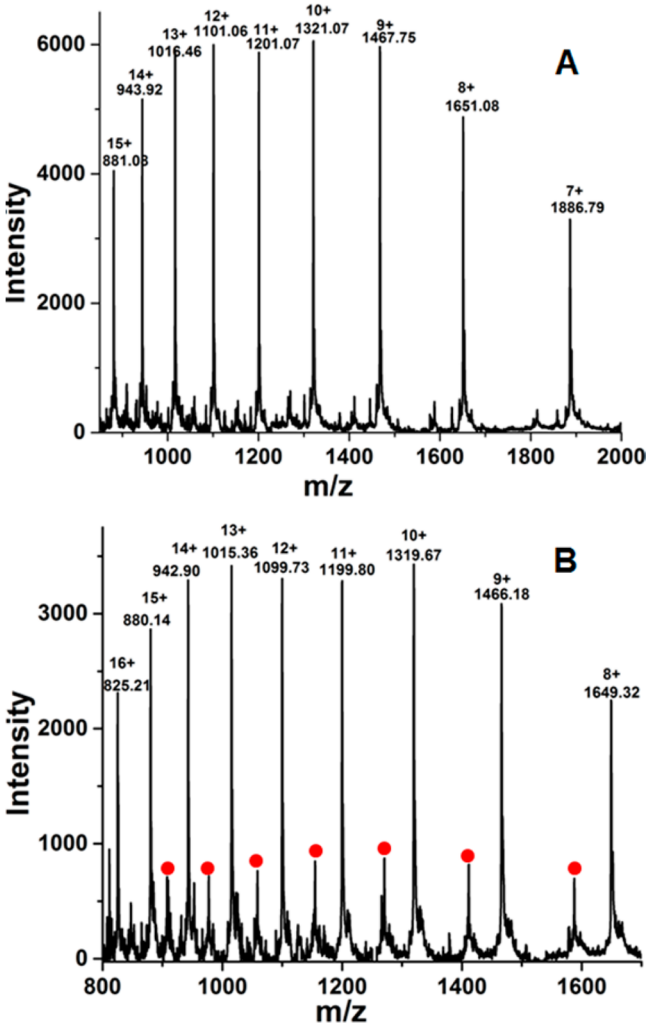

Figure 3. ESI-mass spectra of the semisynthetic WT-NiSOD (A) and H1*NiSOD (B) after the removal of the 2-nitrobenzyl Cys2 protective group by UV irradiation. Peaks under the red dots in B correspond to a modified NΔ5-NiSOD that does not contain a high-affinity nickel binding site.

oxidation (Figure 2A).[28] The synthesis of high purity histidinal in significant quantities and in a form suitable for peptide synthesis is reported here for the first time and was a significant component of the research. It was achieved by protecting the imidazole amine with an adamantyl group prior to reduction of the amino acid and oxidation of the alcohol. Following the removal of the acid-labile protecting groups, NCL was performed as for the semisynthetic WT-NiSOD, except starting with the benzylthioester of the modified pentapeptide. The use of the poorer SBz leaving group compared with NBz used for the WT-NiSOD,[29,30] led to extensive oxidation or desulfurization of the NΔ5-NiSOD N-terminal cysteine when large excesses of TCEP were used,[25] (SI Figure S5) necessitating separation of the desired protein from the impurities that do not contain a thiol by chromatography on activated thiol sepharose. The resulting H1*-NiSOD is ∼70% pure by mass spectral deconvolution. The only remaining impurity is an N-terminally modified NΔ5-NiSOD that does not undergo NCL (SI Figure S6). This species does not affect the characterization of the enzyme because it lacks the high-affinity nickel binding site.

DOI: 10.1021/jacs.5b03629
J. Am. Chem. Soc. 2015, 137, 9044−9052

Following photochemical deprotection of Cys2, the resulting product was analyzed by ESI-MS under denaturing conditions, which confirmed the expected MW for the protein (Figure 3B). The sample was then folded, metalated, and analyzed for Ni content, as described for semisynthetic WT-NiSOD. The sample after chelex treatment was found to be 62% nickel loaded, after taking into account the sample purity. Like the WT enzyme, H1*-NiSOD was also found to be hexameric by size exclusion chromatography (SI Figure S8).

3.2. Structural Characterization of the Ni Site in H1*-NiSOD. XAS analysis was used to characterize the structure of the Ni site in H1*-NiSOD (Figure 4). The XANES spectrum

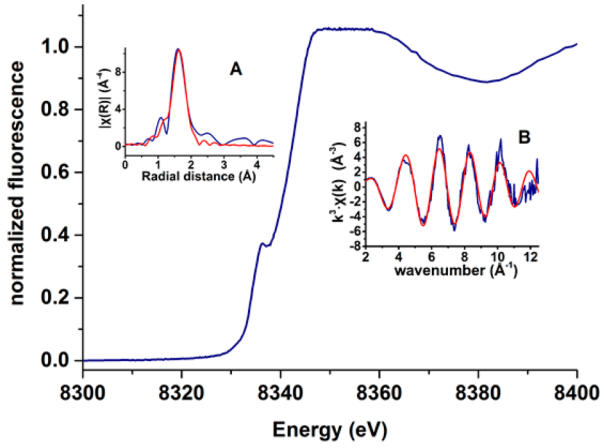

Figure 4. Nickel K-edge XANES spectrum. Inserts: (A) Fourier-transformed (k = 2−12.5 Å^{-1}) EXAFS (blue) and fit (red). (B) k^3, weighted EXAFS data (blue) and fit (red).

shows a resolved maximum near 8336 eV that is associated with a 1s → 4p$_z$ electronic transition that is diagnostic for four-coordinate planar coordination, and is also observed for dithionite-reduced WT-NiSOD[9,31] The expected peak associated with a 1s → 3d transition was not observed; however, it has very low intensity in many 4-coordinate complexes, including some where it is not detected.[31] EXAFS arising from first-coordination sphere scattering atoms was best fit with 2 N-donor atoms @ 1.98(2) Å and 2 S-donor atoms @ 2.14(2) Å (see SI) and is similar to dithionite-reduced WT-NiSOD (Ni—N = 1.91(1) Å; Ni—S = 2.160(4) Å),[9] only with a slightly longer average Ni—N distance, as well as to the distances found in planar NiN_2S_2 complexes (Ni—N = 1.90–1.99 Å; Ni—S = 2.14–2.20 Å).[32,33]

3.3. Electronic Structure. UV−vis absorption spectra of the H1*-NiSOD and semisynthetic WT-NiSOD are compared to spectra obtained for recombinant WT-NiSOD in Figure 5. The semisynthetic WT-NiSOD spectrum closely matches that of the recombinant WT-NiSOD and features the transition near 380 nm that has been assigned to CysS → Ni(III) ligand-to-metal charge transfer (LMCT).[12] This LMCT transition is absent in the spectrum for H1*-NiSOD, which resembles the spectrum obtained for reduced recombinant WT-NiSOD, consistent with the sample being mostly reduced, i.e., Ni(II). EPR spectra obtained on an as-isolated sample of H1*-NiSOD revealed a weak, nearly axial signal that accounts for ∼11% of the nickel in the sample by spin integration. Thus, the resting sample in air contains both Ni(II) and Ni(III) centers, but at a lower Ni(III)/Ni(II) ratio than the recombinant WT enzyme where 50% of the Ni in the aerobic resting enzyme is Ni(III).[8]

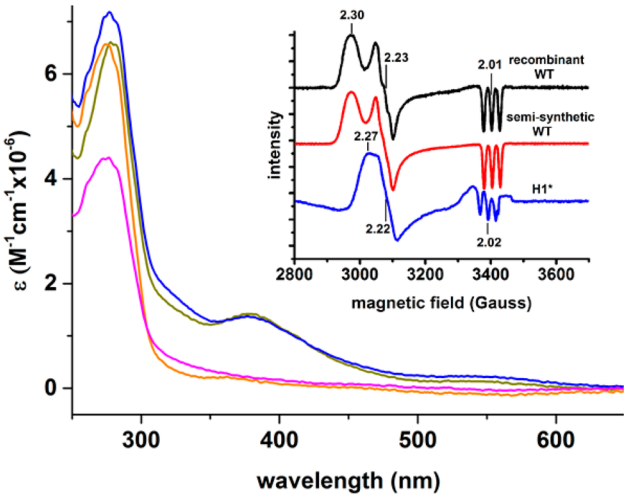

Figure 5. Spectral characterization of semisynthetic NiSODs. UV−vis spectra for as-isolated recombinant WT-NiSOD (green), dithionite-reduced recombinant WT-NiSOD (orange), as-isolated semisynthetic WT-NiSOD (blue), and as-isolated semisynthetic H1*-NiSOD (magenta). Inset: X-band EPR spectra obtained at 77K for as-isolated samples of recombinant WT-NiSOD, semisynthetic WT-NiSOD, and H1*-NiSOD.

The signal has g_x = 2.27, g_y = 2.22, and g_z = 2.02, with hyperfine attributed to the apical His1 imidazole N-donor ligand resolved on g_z, A_{zz} = 24.2 G (Figure 5). This signal is distinct from the rhombic spectrum observed for recombinant WT-NiSOD and semisynthetic WT-NiSOD (g-values =2.30, 2.23, 2.01; A_{zz} = 24.9 G).[8]

3.4. Redox Catalysis. In contrast to the relatively small structural and electronic perturbations, the effect of substitution of the backbone amidate ligand by a secondary amine on redox catalysis is dramatic. Using pulse-radiolytically generated superoxide, the catalytic rate constant determined by monitoring the disappearance of the superoxide radical at 260 nm was only ∼1% of that observed for the recombinant WT-NiSOD. The semisynthetic WT-NiSOD has a catalytic rate constant k_{cat} = 9.4 ± 1.6 × 10^8 M^{-1} s^{-1} at pH = 7.5 and a pH dependence that is experimentally indistinguishable from the catalytic rate constant observed for recombinant WT-NiSOD (Figure 6).[8,34] In contrast, the H1*-NiSOD has a catalytic rate

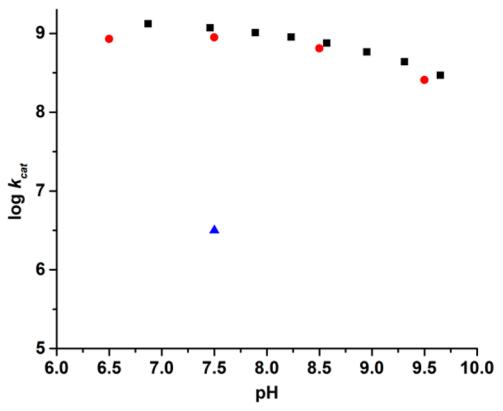

Figure 6. Catalytic activity pH dependence of recombinant WT-NiSOD (black square)[34] compared with that of semisynthetic WT-NiSOD (red circle). The catalytic activity of H1*NiSOD at pH= 7.50 is shown as a blue triangle.

DOI: 10.1021/jacs.5b03629
J. Am. Chem. Soc. 2015, 137, 9044−9052

constant k_{cat} = 5.6 ± 0.5 × 10^6 M^{-1} s^{-1} at pH = 7.5. Nonetheless, this residual activity is due to enzyme catalysis, and not the uncatalyzed bimolecular disproportionation reaction, since doubling the concentration of H1*-NiSOD doubled the rate of reaction (see SI).

4. DISCUSSION

4.1. Synthetic Strategy. The synthetic strategy detailed above provides a method to alter any backbone amide to a secondary amine employing aldehydes derived from amino acids that can be adapted to solid phase peptide synthesis. This approach differs from previous backbone alterations reported in the literature in that it preserves the backbone N atom in the protein, while altering its chemical properties including deprotonation (charge) and ability to engage in π-bonding. Of the strategies for modifying backbone amides that have been employed to make proteins (rather than small peptides), this strategy is novel in that it preserves the N-donor ligand as opposed to replacement with an ester O-donor. The latter can be achieved in several ways including the use of preactivated (L)-lactic acid or (S)-hydroxymethylbutyric acid in solid phase peptide synthesis or the use of α-hydroxyacids in tRNA suppression strategies.[35−42] These amide → ester modifications enabled investigations probing the effect of altering hydrogen bonding interactions involving the amide, but are less applicable to amides that are metal ligands in metalloproteins, since ester O atoms are poor metal ligands. Although rare, metalloenzymes featuring active site metal amidate ligands include nitrile hydratase[43] and thiocyanate hydrolase,[44] in addition to NiSOD studied here. The use of histidinal to modify the peptide bond is specifically applicable to proteins that feature the amino terminal Cu(II)- and Ni(II)-binding (ATCUN) motif,[45] which binds in a tetradentate planar fashion utilizing the N-terminal amine, a histidine residue in position 3, and two intervening amide N atoms. The ATCUN motif is a common feature of albumins, and 95% of serum Ni(II) is bound to albumin.[43] The ATCUN motif is also found in histatins, neuromedins C and K, and human sperm protamine P2a, and is also a component of proteins engineered for DNA cleavage.[43,46−48] N-terminal ATCUN-like binding sites are also features of a number of proteins involved in Ni trafficking, including NmtR,[49] RcnR,[50] and HypA,[51] where the His residue is second residue and the resulting Ni(II) complexes are all six-coordinate.

4.2. NiSOD. The Ni-dependent superoxide dismutases are a large class of superoxide dismutases that are encoded by the *sodN* gene. The *sodN* gene encodes a highly conserved (HCXXPCXXY) N-terminal "nickel hook" motif that binds Ni using the N-terminal amine and the side chain imidazole of His1, the amide N atom and side chain thiolate of Cys2, and the side chain of Cys6 (Figure 1). The N-terminal location of the binding site made synthesis of model peptides an approach that has been extensively exploited for studying the NiSOD active site,[13,14,52,53] and the role of the Cys6 residue as the only ligand not derived from His1 or Cys2 makes semisynthesis of the protein employing NCL very attractive, particularly for a study modifying the backbone amidate ligand, for which no point mutation is possible. Using the synthetic strategy detailed above, histidinal was incorporated into a synthetic pentapeptide in order to produce a variant nickel hook motif, where the amidate ligand of the nickel center in WT-NiSOD was altered to a secondary amine. NCL was then employed to ligate the peptide to the remainder of the enzyme that was produced recombinantly and featured an N-terminal Cys residue.

Taken together, the spectroscopic characterization of H1*-NiSOD suggests that the nickel site in the variant is structurally very similar to those in WT-NiSOD. The Ni(II) sites are four-coordinate and planar with a N_2S_2 ligand donor-atom set, and the Ni(III) sites are five coordinate and pyramidal with the addition of an apical imidazole ligand from His1. Even the electronic structure of the site seems little perturbed in the H1*-NiSOD variant. The EPR spectrum of H1*-NiSOD (g_x = 2.27, g_y = 2.22 and g_z = 2.02, A_{zz} = 24.2 G, Figure 5) is consistent with a low-spin d^7 electronic structure with the unpaired electron residing in a d_z^2 orbital, similar to WT-NiSOD, but has a more axial signal than the rhombic signal observed for WT-enzyme. This arises mostly from a shift of g_x from 2.30 to 2.27 in the variant. This can be rationalized in terms of the interaction of the N-donors with π-symmetry orbitals on the Ni(III) center. An amidate N-donor is expected to raise the energy of a π-symmetry Ni 3d orbital through a filled $\pi-\pi$ interaction that is not present for an amine N-donor (Figure 7).[12] Thus, asymmetric amidate−amine ligation would affect interactions with d_{xz} and d_{yz} differently, and is reflected in a rhombic EPR signal.

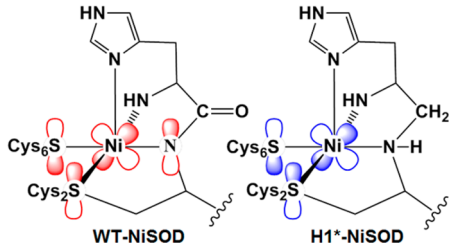

Figure 7. NiSOD active site diagrams illustrating the different interactions between the N-donor ligands and a Ni π-symmetry 3d orbital in WT-NiSOD with a Cys2 amidate ligand (left), and in H1*-NiSOD with a Cys2 2° amine (right).

Despite the minor structural and electronic perturbations, the alteration of the Cys2 amidate ligand to a secondary amine in H1*-NiSOD has a dramatic effect on the redox catalytic properties of the active site. Alteration of the amidate ligand found in WT-NiSOD to a secondary amine apparently results in raising the redox potential of the nickel site to a value that is less accessible to air oxidation, resulting in lower amounts of Ni(III) in as-isolated samples of H1*-NiSOD (11%) relative to recombinant WT-NiSOD (50%) and is accompanied by lower catalytic activity. Assuming Nerstian behavior, and given that the E^0 value of WT-NiSOD is ∼0.29 V vs NHE,[8] H1*NiSOD is calculated to have an E^0 ≈ 0.35 V. The general decrease in activity associated with an increase in redox potential is in line with expectations based on studies of other mutants. For example, D3A-NiSOD has an E^0 ≈ 0.31 V, and catalytic activity that is reduced to ∼30% of WT-NiSOD.[8] The higher calculated redox potential for H1*-NiSOD would be expected to greatly decrease the catalytic activity, in line with the observed activity of 1% of WT-NiSOD. In addition, the trend for increased redox potentials in amine complexes relative to complexes with amidate ligands has been noted.[54,55] The increased redox potential makes Ni(III) harder to access and thus inhibits the reduction of O_2^- to H_2O_2. Thus, the single amidate ligand present in the WT-NiSOD plays a critical role in the redox tuning of the catalytic site. A detailed comparison of the electronic structures and redox properties of the variant and

DOI: 10.1021/jacs.5b03629
J. Am. Chem. Soc. 2015, 137, 9044−9052

WT-enzyme await the results of DFT computations currently in progress.

■ ASSOCIATED CONTENT

Supporting Information

Tables of reaction rates and EXAFS and XANES analysis. Amino acid sequence of the pelB WT-NiSOD. Schematic diagram for the NΔ5-NiSOD chemical rescue. Figures describing ESI-MS data on intermediates. Size exclusion chromatography. The Supporting Information is available free of charge on the ACS Publications website at DOI: 10.1021/jacs.5b03629.

■ AUTHOR INFORMATION

Corresponding Author

*mmaroney@chem.umass.edu

Author Contributions

The manuscript was written through contributions of all authors. All authors have given approval to the final version of the manuscript.

Notes

The authors declare no competing financial interest.

■ ACKNOWLEDGMENTS

This work was supported by a grant from the National Science Foundation (CHE-0809188 to M.J.M.). Portions of this research were carried out at the Stanford Synchrotron Radiation Laboratory, a national user facility operated by Stanford University on behalf of the U.S. Department of Energy, Office of Basic Energy Sciences. The SSRL Structural Molecular Biology Program is supported by the Department of Energy, Office of Biological and Environmental Research, and by the National Institutes of Health. The kinetic studies conducted at Brookhaven National Laboratory were carried out at the Accelerator Center for Energy Research, which is supported by the US DOE Office of Science, Division of Chemical Sciences, Geosciences and Biosciences under Contract N°. DE-AC02-98CH10886. We gratefully acknowledge the gift of Fmoc-*S*-*o*-nitrobenzyl cysteine from Dr. James J. Chambers and the design of the pelB WT-NiSOD plasmid by Carolyn Carr. The authors also acknowledge helpful discussions regarding NCL with Dr. Philip Dawson, and thank Dr. Michael Hendrich for providing his SpinCount EPR simulation software.

■ REFERENCES

(1) Keele, B. B., Jr; McCord, J. M.; Fridovich, I. *J. Biol. Chem.* **1970**, *245*, 6176−6181.
(2) Sheng, Y.; Abreu, I. A.; Cabelli, D. E.; Maroney, M. J.; Miller, A.; Teixeira, M.; Valentine, J. S. *Chem. Rev.* **2014**, *114*, 3854−3918.
(3) Cadenas, E.; Davies, K. J. *Free Radical Biol. Med.* **2000**, *29*, 222−230.
(4) Winterbourn, C. C. *Free Radical Biol. Med.* **1993**, *14*, 85−90.
(5) Youn, H.; Kim, E.; Roe, J.; Hah, Y.; Kang, S. *Biochem. J.* **1996**, *318*, 889−896.
(6) Bryngelson, P. A.; Arobo, S. E.; Pinkham, J. L.; Cabelli, D. E.; Maroney, M. J. *J. Am. Chem. Soc.* **2004**, *126*, 460−461.
(7) Abreu, I. A.; Cabelli, D. E. *Biochim. Biophys. Acta, Proteins Proteomics* **2010**, *1804*, 263−274.
(8) Herbst, R. W.; Guce, A.; Bryngelson, P. A.; Higgins, K. A.; Ryan, K. C.; Cabelli, D. E.; Garman, S. C.; Maroney, M. J. *Biochemistry* **2009**, *48*, 3354−3369.
(9) Choudhury, S. B.; Lee, J.; Davidson, G.; Yim, Y.; Bose, K.; Sharma, M. L.; Kang, S.; Cabelli, D. E.; Maroney, M. J. *Biochemistry* **1999**, *38*, 3744−3752.
(10) Wuerges, J.; Lee, J. W.; Yim, Y. I.; Yim, H. S.; Kang, S. O.; Djinovic Carugo, K. *Proc. Natl. Acad. Sci. U. S. A.* **2004**, *101*, 8569−8574.
(11) Barondeau, D. P.; Kassmann, C. J.; Bruns, C. K.; Tainer, J. A.; Getzoff, E. D. *Biochemistry* **2004**, *43*, 8038−8047.
(12) Fiedler, A. T.; Bryngelson, P. A.; Maroney, M. J.; Brunold, T. C. *J. Am. Chem. Soc.* **2005**, *127*, 5449−5462.
(13) Shearer, J.; Long, L. M. *Inorg. Chem.* **2006**, *45*, 2358−2360.
(14) Neupane, K. P.; Shearer, J. *Inorg. Chem.* **2006**, *45*, 10552−10566.
(15) Mullins, C.; Grapperhaus, C.; Kozlowski, P. *JBIC, J. Biol. Inorg. Chem.* **2006**, *11*, 617−625.
(16) Shearer, J.; Dehestani, A.; Abanda, F. *Inorg. Chem.* **2008**, *47*, 2649−2660.
(17) Grapperhaus, C. A.; Maguire, M. J.; Tuntulani, T.; Darensbourg, M. Y. *Inorg. Chem.* **1997**, *36*, 1860−1866.
(18) Mirza, S. A.; Pressler, M. A.; Kumar, M.; Day, R. O.; Maroney, M. J. *Inorg. Chem.* **1993**, *32*, 977−987.
(19) Grapperhaus, C. A.; Darensbourg, M. Y. *Acc. Chem. Res.* **1998**, *31*, 451−459.
(20) Kaasjager, V. E.; Bouwman, E.; Gorter, S.; Reedijk, J.; Grapperhaus, C. A.; Reibenspies, J. H.; Smee, J. J.; Darensbourg, M. Y.; Derecskei-Kovacs, A.; Thomson, L. M. *Inorg. Chem.* **2002**, *41*, 1837−1844.
(21) Gentle, I. E.; De Souza, D. P.; Baca, M. *Bioconjugate Chem.* **2004**, *15*, 658−663.
(22) Fauvet, B.; Fares, M. B.; Samuel, F.; Dikiy, I.; Tandon, A.; Eliezer, D.; Lashuel, H. A. *J. Biol. Chem.* **2012**, *287*, 28243−28262.
(23) Stevens, C. M.; Watanabe, R. *J. Am. Chem. Soc.* **1950**, *72*, 725−727.
(24) Okada, Y.; Wang, J.; Yamamoto, T.; YOKOI, T.; MU, Y. *Chem. Pharm. Bull.* **1997**, *45*, 452−456.
(25) Wang, Z.; Rejtar, T.; Zhou, Z. S.; Karger, B. L. *Rapid Commun. Mass Spectrom.* **2010**, *24*, 267−275.
(26) Leitch, S.; Bradley, M. J.; Rowe, J. L.; Chivers, P. T.; Maroney, M. J. *J. Am. Chem. Soc.* **2007**, *129*, 5085−5095.
(27) Martin-Diaconescu, V.; Bellucci, M.; Musiani, F.; Ciurli, S.; Maroney, M. J. *JBIC, J. Biol. Inorg. Chem.* **2012**, *17*, 353−361.
(28) Myers, A. G.; Zhong, B.; Movassaghi, M.; Kung, D. W.; Lanman, B. A.; Kwon, S. *Tetrahedron Lett.* **2000**, *41*, 1359−1362.
(29) Dawson, P. E.; Churchill, M. J.; Ghadiri, M. R.; Kent, S. B. *J. Am. Chem. Soc.* **1997**, *119*, 4325−4329.
(30) Blanco-Canosa, J. B.; Dawson, P. E. *Angew. Chem., Int. Ed.* **2008**, *47*, 6851−6855.
(31) Colpas, G. J.; Maroney, M. J.; Bagyinka, C.; Kumar, M.; Willis, W. S.; Suib, S. L.; Mascharak, P. K.; Baidya, N. *Inorg. Chem.* **1991**, *30*, 920−928.
(32) Smee, J. J.; Miller, M. L.; Grapperhaus, C. A.; Reibenspies, J. H.; Darensbourg, M. Y. *Inorg. Chem.* **2001**, *40*, 3601−3605.
(33) Grapperhaus, C. A.; Mullins, C. S.; Mashuta, M. S. *Inorg. Chim. Acta* **2005**, *358*, 623−632.
(34) Ryan, K. C.; Johnson, O. E.; Cabelli, D. E.; Brunold, T. C.; Maroney, M. J. *JBIC, J. Biol. Inorg. Chem.* **2010**, *15*, 795−807.
(35) Koh, J. T.; Cornish, V. W.; Schultz, P. G. *Biochemistry* **1997**, *36*, 11314−11322.
(36) Shin, I.; Ting, A. Y.; Schultz, P. G. *J. Am. Chem. Soc.* **1997**, *119*, 12667−12668.
(37) Low, D. W.; Hill, M. G. *J. Am. Chem. Soc.* **2000**, *122*, 11039−11040.
(38) Jude, A. R.; Providence, L. L.; Schmutzer, S. E.; Shobana, S.; Greathouse, D. V.; Andersen, O. S.; Koeppe, R. E. *Biochemistry* **2001**, *40*, 1460−1472.
(39) Lu, W.; Qasim, M.; Laskowski, M.; Kent, S. B. *Biochemistry* **1997**, *36*, 673−679.

DOI: 10.1021/jacs.5b03629
J. Am. Chem. Soc. 2015, 137, 9044−9052

(40) Eildal, J. N.; Hultqvist, G.; Balle, T.; Stuhr-Hansen, N.; Padrah, S.; Gianni, S.; Strømgaard, K.; Jemth, P. *J. Am. Chem. Soc.* **2013**, *135*, 12998−13007.
(41) Baca, M.; Kent, S. B. *Tetrahedron* **2000**, *56*, 9503−9513.
(42) Bain, J.; Diala, E. S.; Glabe, C. G.; Wacker, D. A.; Lyttle, M. H.; Dix, T. A.; Chamberlin, A. R. *Biochemistry* **1991**, *30*, 5411−5421.
(43) Harrop, T. C.; Mascharak, P. K. *Acc. Chem. Res.* **2004**, *37*, 253−260.
(44) Arakawa, T.; Kawano, Y.; Kataoka, S.; Katayama, Y.; Kamiya, N.; Yohda, M.; Odaka, M. *J. Mol. Biol.* **2007**, *366*, 1497−1509.
(45) Harford, C.; Sarkar, B. *Acc. Chem. Res.* **1997**, *30*, 123−130.
(46) Mack, D. P.; Iverson, B. L.; Dervan, P. B. *J. Am. Chem. Soc.* **1988**, *110*, 7572−7574.
(47) Mack, D. P.; Dervan, P. B. *J. Am. Chem. Soc.* **1990**, *112*, 4604−4606.
(48) Mack, D. P.; Dervan, P. B. *Biochemistry* **1992**, *31*, 9399−9405.
(49) Reyes-Caballero, H.; Lee, C. W.; Giedroc, D. P. *Biochemistry* **2011**, *50*, 7941−7952.
(50) Iwig, J. S.; Leitch, S.; Herbst, R. W.; Maroney, M. J.; Chivers, P. T. *J. Am. Chem. Soc.* **2008**, *130*, 7592−7606.
(51) Herbst, R. W.; Perovic, I.; Martin-Diaconescu, V.; O'Brien, K.; Chivers, P. T.; Pochapsky, S. S.; Pochapsky, T. C.; Maroney, M. J. *J. Am. Chem. Soc.* **2010**, *132*, 10338−10351.
(52) Shearer, J.; Neupane, K. P.; Callan, P. E. *Inorg. Chem.* **2009**, *48*, 10560−10571.
(53) Neupane, K. P.; Gearty, K.; Francis, A.; Shearer, J. *J. Am. Chem. Soc.* **2007**, *129*, 14605−14618.
(54) Mathrubootham, V.; Thomas, J.; Staples, R.; McCraken, J.; Shearer, J.; Hegg, E. L. *Inorg. Chem.* **2010**, *49*, 5393−5406.
(55) Shearer, J.; Zhao, N. *Inorg. Chem.* **2006**, *45*, 9637−9639.

DOI: 10.1021/jacs.5b03629
J. Am. Chem. Soc. 2015, 137, 9044−9052